

ORIGINAL RESEARCH

Intra-cheek immunization as a novel vaccination route for therapeutic vaccines of head and neck squamous cell carcinomas using plasmid virus-like particles

Rodney Macedo^a, Juliette Rochefort^{a,b}, Maude Guillot-Delost^a, Kae Tanaka^a, Aline Le Moignic^a, Clara Noizat^a, Claude Baillou^a, Véronique Mateo^a, Antoine F. Carpentier^c, Eric Tartour^d, Chloé Bertolus^{a,e}, Bertrand Bellier^f, Géraldine Lescaille^{a,b,*}, and François M. Lemoine^{a,g,*}

^aSorbonne Universités, UPMC/Paris 06, UMR-S INSERM U1135, CNRS ERL 8255, Center d'Immunologie et Maladies Infectieuses (CIMI-Paris), Paris, France; ^bParis Diderot/Paris 07, Sorbonne Paris Cité, Assistance Publique-Hôpitaux de Paris (AP-HP), Groupe hospitalier Pitié-Salpêtrière, Department of Odontology, Paris, France; ^cUniversité Paris 13, AP-HP, Hôpital Avicenne, Department of Neurology, Bobigny, France; ^dParis Descartes/Paris 05, Sorbonne Paris Cité, INSERM U970, Paris-Cardiovascular Research Center (PARC), AP-HP, Hôpital Européen Georges Pompidou, Service d'Immunologie Biologique, Paris, France; ^eSorbonne Universités, UPMC Univ-Paris 06, AP-HP, Groupe hospitalier Pitié-Salpêtrière, Department of Maxillofacial Surgery, Paris, France; ^fSorbonne Universités, UPMC/Paris 06, UMR-S INSERM U959, CNRS, FRE 3632, Immunology-Immunopathology-Immunotherapy (I3), Paris, France; ^gAP-HP, Groupe Hospitalier Pitié-Salpêtrière, Department of Biotherapies, Paris, France

ABSTRACT

Despite current therapy, head and neck squamous cell carcinomas (HNSCCs) arising from various mucosal sites of the upper aero-digestive tract frequently relapse in a loco-regional manner and have a poor prognosis. Our objective was to validate an innovative mucosal route of vaccination using plasmid virus-like particles (pVLPs) in a pre-clinical orthotopic model of HNSCCs. For this purpose, we used pVLP-E7, that are plasmid DNA encoding retroviral virus-like particles carrying a truncated E7 oncoprotein from HPV-16 as antigen model, to vaccinate mice bearing pre-established TC-1 tumors implanted into the buccal mucosa. pVLP-E7 were combined with clinical grade TLR agonists (Imiquimod and CpG-ODN). In this pre-clinical orthotopic model, whose tumor microenvironment resembles to those of human HNSCCs, different mucosal vaccination routes were tested for their ability to elicit efficient immune and antitumoral responses. Results showed that mucosal intra-cheek (IC) vaccinations using pVLP-E7, comparatively to intradermic vaccinations (ID), gave rise to higher mobilization of mucosal (CD49a⁺) CD8⁺ specific effector T cells in both tumor draining lymph nodes (TdLNs) and tumor microenvironment resulting in better antitumor effects and in a long-term protection against tumor rechallenge. *In vivo* CD8⁺ depletion demonstrated that antitumoral effects were fully dependent upon the presence of CD8⁺ T cells. Validation of IC mucosal vaccinations with pVLPs combined with adjuvants using a pre-clinical orthotopic model of HNSCC provides valuable pre-clinical data to rapidly envision the use of such therapeutic vaccines in patients with HNSCCs, inasmuch as vaccinal components and adjuvants can be easily obtained as clinical grade reagents.

Abbreviations: ALN, axillary lymph nodes; CH, cheek model; CLN, cervical lymph nodes; DC, dendritic cells; HNSCC, head and neck squamous cell carcinomas; HPV, human papillomavirus; IC, intra-cheek; ID, intradermic; IFN γ , interferon- γ ; ILN, inguinal lymph nodes; IMQ, Imiquimod; IN, intranasal; NK, natural killer cells; OSCCs, oral cavity squamous cell cancer; pVLPs, plasmid virus-like particles; SC, subcutaneous model; TdLNs, tumor draining lymph nodes; TLR, Toll-like receptors; Treg, regulatory T-cells

ARTICLE HISTORY

Received 30 November 2015
Revised 26 February 2016
Accepted 7 March 2016

KEYWORDS

Head and neck squamous cell carcinomas; intra-cheek route; mucosal immunization; pre-clinical orthotopic model; plasmid virus-like particles; tumor microenvironment; therapeutic vaccines

Introduction

HNSCCs represent the sixth most frequent type of cancer in the world with global incidence and mortality rates annually estimated at 540,000 and 270,000 cases, respectively.¹ HNSCCs are anatomically and clinically heterogeneous and arise from the mucosal surface of the oral cavity (OSCC), oropharynx (OPSCC), hypopharynx, larynx, sinuses and other sites within the upper aero-digestive tract. Traditionally, HNSCCs are associated with alcohol and tobacco abuse.² However, there is an increased incidence of HNSCCs occurring in younger population without exposure to these chemical carcinogens,³ especially

in OSCCs and OPSCCs. Moreover, OPSCCs are frequently associated to human papillomavirus type-16 (HPV-16).⁴ Standard treatments for HNSCCs combine surgery, radiation and chemotherapy depending upon the site of the disease and the degree of invasion and metastases. However, HNSCCs are very challenging to treat, and 35% to 55% of patients develop loco-regional or metastatic recurrence within 2 y. Thus, the prognosis of these patients remains poor, with a survival rate of less than 10–20% at 10 y.⁵ Thus, there is an urgent need to develop innovative therapies for HNSCCs.

CONTACT Prof. François M. Lemoine ✉ francois.lemoine@upmc.fr; Dr. Géraldine Lescaille ✉ geraldine.lescaille@gmail.com

Supplemental data for this article can be accessed on the publisher's website.

*Equal contribution as senior authors.

© 2016 Taylor & Francis Group, LLC

In a previous published report,⁶ we have developed an experimental strategy of therapeutic vaccines based on the use of plasmid DNA encoding retrovirus-like particles (pVLPs), an approach that combines DNA vaccination and VLP formation, to treat TC-1 tumor-bearing mice. Indeed, TC-1 cells, which over-express E6 and E7 oncoproteins from HPV-16, were subcutaneously (SC) implanted into the flank of animals. When tumors were well established, mice were ID vaccinated with pVLP harboring a non-oncogenic mutated E7 protein (pVLP-E7). Injection of pVLPs was associated with local electroporation in order to improve the immunization efficiency. We first showed that the pVLP strategy was more efficient than DNA vaccination or VLP alone to induce antigen-specific immune responses and antitumor effects. Thus, therapeutic vaccinations with pVLP-E7, when combined with TLR agonists such as CpG-ODN and Imiquimod, were able to control the growth of advanced tumors and to cure 50% of the mice resulting in a long-term disease free survival.

Although these data are encouraging, the ectopic model used is not adequate as a pre-clinical model for HNSCCs, making it difficult to extrapolate the efficacy of therapeutic vaccines using pVLPs. Thus, an orthotopic tumor model that recapitulates HNSCC characteristics must be developed. Furthermore, considering the mucosal origin of these cancers and the necessity to generate better loco-regional responses, it might be of interest to test different mucosal vaccination routes. Indeed, it has been shown that mucosal immunizations are more efficient to selectively elicit antitumor specific T-cell responses against mucosal tumors.⁷ In order to address these questions, we first validated an orthotopic tumor model consisting of infusing tumor cells into the CH of animals, and then we evaluated different mucosal immunizations routes using pVLPs. Our findings showed that mucosal IC vaccinations using pVLP-E7, as compared to ID vaccination, gave rise to a higher mobilization of CD8⁺ specific T cells in TdLNs and in the tumor environment resulting in better antitumor effects and in a long-term protection.

Results

Validation of an orthotopic tumor model for oral squamous cell carcinomas

In order to develop an orthotopic murine tumor model that shares anatomical and cellular features of human HNSCC, we first evaluated by multiparametric flow-cytometry (Fig. 1A) the inflammatory cellular components of OSCC microenvironment comparatively to healthy gingiva. Analysis of tumor microenvironment showed significant increases of total CD45⁺ cells (Fig. 1B, left panel), granulocytes, macrophages, myeloid (mDC) and plasmacytoid dendritic cells (pDC), and T lymphocyte subsets, albeit not B lymphocytes (Fig. 1B upper right panel). Furthermore, these increases in absolute cell counts were accompanied by higher percentages of mDC, macrophages and regulatory T cells (Treg) within gated CD45⁺ cells (Fig. 1B, lower right panel). Thus, these data underlined the presence of inflammatory cells and adaptive immune cells within the tumor microenvironment of OSCCs.

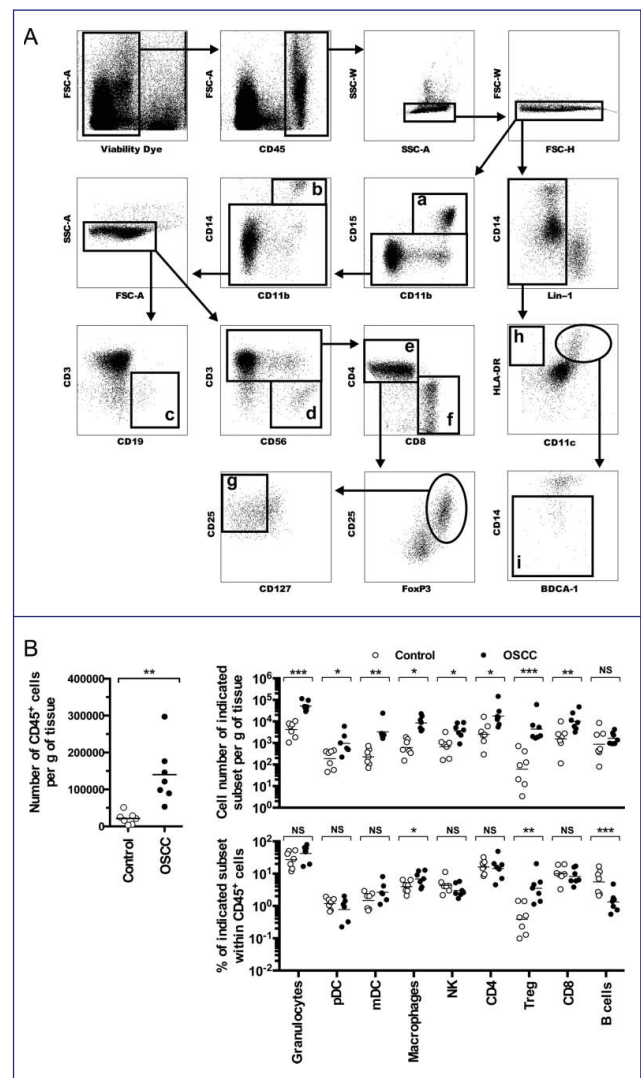


Figure 1. Human Oral Squamous Cell Carcinomas are inflammatory neoplasms. Single cell suspensions were obtained from human OSCC samples ($n = 7$) and healthy gingiva ($n = 7$), and analyzed by flow cytometry. (A) Gating strategy: after dead cells and doublets exclusion, nine subpopulations were identified within CD45⁺ cells: (a) CD15⁺CD11b⁺ (granulocytes), (b) CD14⁺CD11b⁺ (macrophages), (c) CD19⁺CD3⁻ (B cells), (d) CD56⁺CD3⁻ (Natural Killer cells), (e) CD3⁺CD4⁺ (CD4⁺ T cells), (f) CD3⁺CD8⁺ (CD8⁺ T cells), (g) CD3⁺CD4⁺CD25⁺FoxP3⁺CD127⁻ (Treg), (h) Lin-1neg (CD3⁻CD19⁻CD56⁻) HLA-DR⁺CD11c⁻ (pDC) and (i) Lin-1negCD-11c⁺HLA-DR⁻CD14⁻ (mDC). (B) Number of CD45⁺ cells per gram (g) of tissue (left panel), cell number of indicated subset per g of tissue (upper right panel) and percent of indicated subset within CD45⁺ cells (lower right panel) are presented. NS, non-statistical difference = $p > 0.05$; * $p < 0.05$; ** $p < 0.01$; *** $p < 0.001$.

Secondly, we designed two orthotopic murine models using TC-1-Luc cells where cells were infused into the tongue intra-lingual (IL) or in the submucosal lining of the CH. These models were compared to subcutaneous ectopic tumors (SC) growing in the flank of animals (Fig. 2A left panel). Survival curves (Fig. 2A right panel) indicate that the IL group had the worse survival rate in comparison to other groups. Indeed, IL tumor-bearing mice had to be euthanized earlier because of tumor growth preventing correct feeding. Mice bearing CH tumors could be kept alive for a significant longer time than the IL model, albeit slightly shorter than the SC ectopic model.

Whether or not CH (orthotopic) and SC (ectopic) tumor models display different tumor microenvironment depending

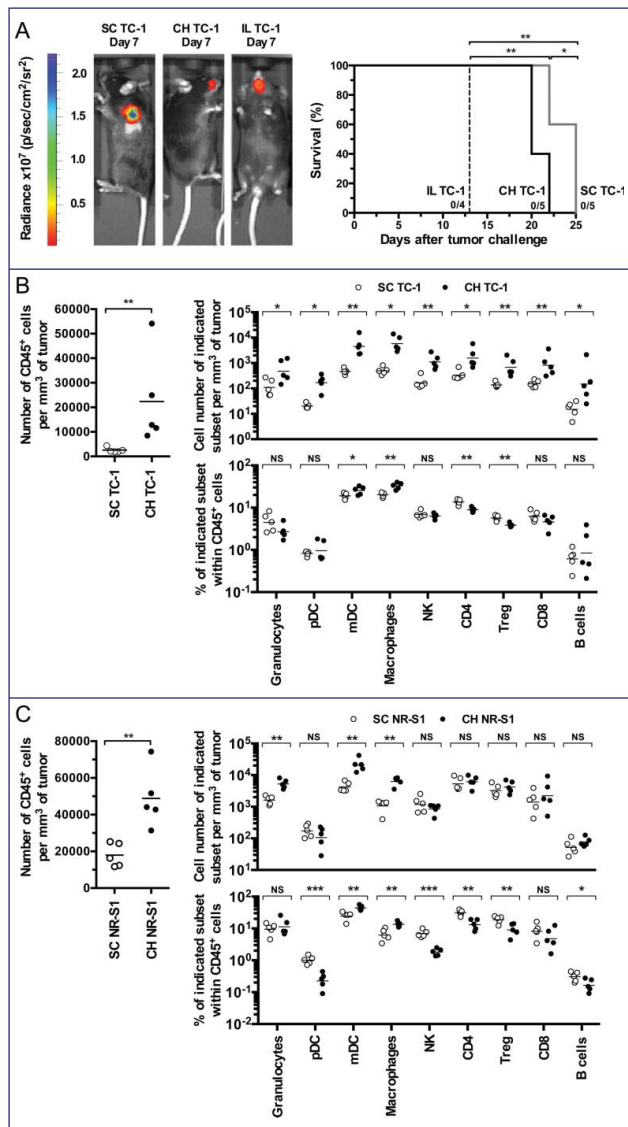


Figure 2. Orthotopic tumor models for OSCCs. C57BL/6 mice (5 mice per group) were injected with TC-1-Luc cells using subcutaneous (SC), intra-cheek (CH) or intra-lingual (IL) routes. (A) A representative bioluminescence imaging is shown one-week after TC-1-Luc injection (left panel). Kaplan–Meier curves show tumor-specific survival rates (right panel). (B) Flow cytometry analysis of cell suspensions from tumors obtained two weeks after TC-1-Luc cell injection in C57BL/6 mice (5 mice per group). For gating strategy, see Fig. S1. Number of CD45⁺ cells per mm³ of tumor (left panel), cell number of indicated subset per mm³ of tumor (upper right panel) and percent of indicated subset within CD45⁺ cells (lower right panel) are presented. (C) Flow cytometry analysis of cell suspensions from tumors obtained two weeks after injection of NR-S1 cells using SC and IC routes in C3H mice (5 mice per group). Number of CD45⁺ cells per mm³ of tumor (left panel), cell number of indicated subset per mm³ of tumor (upper right panel) and percent of indicated subset within CD45⁺ cells (lower right panel) are shown. NS, non-statistical difference = $p > 0.05$; * $p < 0.05$; ** $p < 0.01$; *** $p < 0.001$; **** $p < 0.0001$.

upon the tumor localization was further examined by using multiparametric flow cytometry (see Fig. S1 for gating strategy). Thus, cell suspensions from tumors, TdLNs and spleens were analyzed at day 13 after tumor challenge. Results showed a significant increase of total CD45⁺ cells in tumors from the CH orthotopic model, as compared to those from the ectopic SC model (Fig. 2B, left panel). This significant increase was also observed in TdLNs but not in the spleen (Fig. S2). Analysis of innate and adaptive cells in tumors showed a significant increase of granulocytes and macrophages, mDCs and pDCs,

NK cells, T-cell subsets (CD4⁺ cells, CD8⁺ cells, Treg) and B-cells in the CH orthotopic model, as compared to the ectopic SC model (Fig. 2B, upper right panel). Interestingly, this increase was also accompanied by higher percentages of mDCs and macrophages within gated CD45⁺ cells as observed in the microenvironment of OSCCs (Fig. 2B, lower right panel). To better validate the orthotopic tumor model and eliminate a bias due to the fact that TC-1-Luc cells are genetically modified lung epithelial cells, we have also injected NR-S1 cells,⁸ an oral squamous cell carcinoma cell line which do not express HPV-16 oncoproteins or luciferase, either SC or into the CH of mice. As observed for TC-1-Luc tumors, a significant global infiltration of adaptive and innate cells was found in the CH orthotopic NR-S1 model, as compared to the ectopic SC NR-S1 model (Fig. 2C, left and upper right panels). Again, higher percentages of mDCs and macrophages within gated CD45⁺ cells were observed (Fig. 2B, lower right panel). These findings indicate that IC infusions of either TC-1-Luc cells or NR-S1 cells gave rise to more inflammatory tumor microenvironments that may be related to the peculiar anatomic localization and mucosal development of these tumors, as observed for OSCCs in humans. Thus, the CH orthotopic model appears as a suitable model for mimicking OSCCs.

Advantage of intra-cheek vaccinations for inducing local and loco-regional antigen-specific CD8⁺ T-cell responses in tumor-bearing mice

Because OSCCs originated from the mucosa and frequently relapse locally, it might be important to compare different vaccination routes in view of eliciting local and systemic immunity. For this purpose, we immunized naive mice at day 0, 2 and 4 with pVLP-E7 using three different routes: intradermal (ID), intranasal (IN) and IC. Anti-E7 CD8⁺ responses were assessed by IFN γ ELISpot assay in draining lymph nodes (dLNs), in the spleen, and in non-draining lymph nodes (ndLNs) of different groups of mice (immunized or not), one week after the last immunization (Fig. 3A). Results showed that ID immunizations gave rise to highly significant ($p < 0.0001$) E7-specific CD8⁺ T-cell responses in dLNs (inguinal LNs) and in the spleen, but no response ($p > 0.05$) in ndLNs (cervical LNs). Likewise, IC immunizations gave rise to high CD8⁺ T-cell responses ($p < 0.0001$) in dLNs (cervical LNs) and in the spleen, but no significant CD8⁺ responses in ndLNs (inguinal LNs). After IN immunizations, no significant responses could be observed in any of the LNs or spleens studied. These data indicate that the IC vaccination route is as effective as the ID vaccination route to elicit loco-regional and systemic antigen-specific responses. Because polypeptide E7 vaccinations in combination with adjuvant (CpG-ODN) have been proposed to treat HPV-related cancers, we wondered whether IC or ID vaccination routes using pVLP-E7 could or not elicit better CD8⁺ responses in dLNs as compared to polypeptide E7 (E7). Results showed that both IC and ID pVLP-E7 immunizations significantly elicited higher numbers of E7-specific CD8⁺ T cells than polypeptide E7 immunizations in dLNs (Fig. 3B).

We further addressed whether the vaccination route may induce or not a different antitumor effect in mice bearing TC-1-Luc orthotopic tumors. Thus, mice were vaccinated either ID

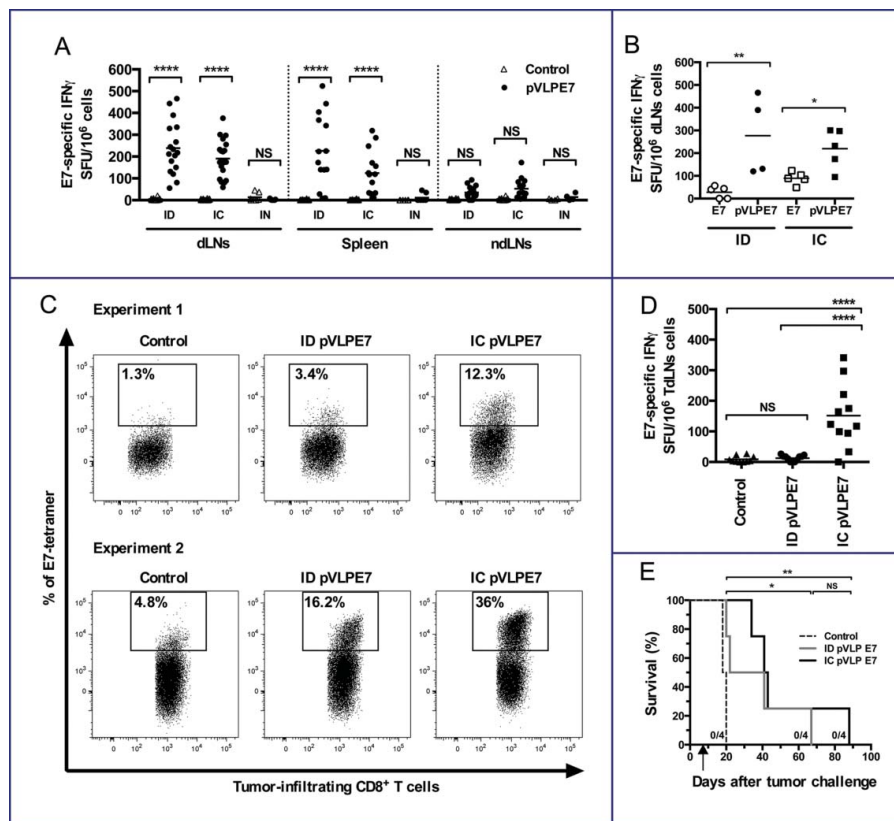


Figure 3. Advantage of intra-cheek vaccinations for inducing local and loco-regional antigen-specific CD8⁺ T-cell responses in tumor-bearing mice. (A) IFN γ ELISpot assay performed at day 10 using cell suspensions from draining lymph nodes (dLNs), spleen and non-draining lymph nodes (ndLNs), C57BL/6 mice being immunized at days 0–2–4 with pVLP-E7 using intra-dermal (ID), intra-cheek (IC) or intranasal (IN) routes of vaccination. Data were obtained from three separate experiments using 4–6 mice per group. (B) IFN γ ELISpot assay performed at day 10 using cell suspensions from dLNs, C57BL/6 mice (4–5 mice) being immunized at days 0–2–4 with pVLP-E7 or E7 polypeptide (+ CpG-ODN) using the ID or IC route. (C) and (D) C57BL/6 mice were injected in the cheek with TC-1-Luc cells, and then ID or IC immunized with pVLP-E7 at days 7–9–11 following tumor challenge. (C) Detection of E749-57-specific CD8⁺ T cells: cell suspensions from tumors were pooled from either 5 mice (Experiment 1) or 6 mice (Experiment 2) and stained with E7-tetramers at day 18. Data obtained from Experiment 1 (5 mice pooled) and Experiment 2 (6 mice pooled). (D) IFN γ ELISpot assay performed using cell suspensions from tumor draining lymph nodes (TdLNs) cells at day 18. Presented data are pooled from two separate experiments (5 and 6 mice per group). (E) Kaplan–Meier curves showing tumor-free survival rates. For ELISpot assays, cells were loaded and stimulated with E749-57 peptide. Background (always ≤ 100 spots per 10^6 cells) obtained with not pulsed cells was subtracted due to some variability between the different tissues tested. NS, non-statistical difference = $p > 0.05$; * $p < 0.05$; ** $p < 0.01$; *** $p < 0.001$; **** $p < 0.0001$.

or IC with pVLP-E7 at days 7–9–11 following tumor cell infusion. IC vaccinations were performed onto the contro-lateral side of the CH orthotopic tumors. Analysis of tumor cell suspensions obtained 7 d after vaccinations revealed higher percentages of H-2Db/E7 tetramer⁺ CD8⁺ T cells within tumor microenvironment of mice vaccinated by IC route comparatively to ID route (Fig. 3C). Moreover, analysis of anti-E7 CD8⁺ responses by IFN γ ELISpot assay in TdLNs showed that IC vaccinations gave rise to significantly higher specific CD8⁺ T-cell responses ($p < 0.0001$) than ID vaccinations (Fig. 3D). Whether IC vaccinations may have a better therapeutic effect than ID vaccinations was further studied. Mice grafted with TC-1-Luc cells using the CH orthotopic model were IC or ID vaccinated with pVLP-E7 at days 7–9–11 after tumor cell infusion. A decrease of the tumor growth was observed comparatively to untreated mice after pVLP-E7 vaccinations using both routes, resulting in a significant prolonged survival (Fig. S3 and Fig. 3E). However, no complete tumor regression could be observed after either IC or ID vaccinations, and all mice were euthanized. Altogether, our results show that IC vaccinations are superior over ID vaccinations for eliciting local and loco-regional immune responses in tumor-bearing mice.

Nonetheless, no curative effect was observed with pVLP-E7 alone using either the IC or ID route of vaccination.

Therapeutic advantage of intra-cheek vaccinations when combined with adjuvants

Although IC immunizations gave rise to better specific immune responses than ID vaccinations, no major therapeutic effect was observed. We have previously described that pVLP-E7 vaccine administrated by ID route in combination with adjuvants such as Imiquimod and CpG-ODN, which act as TLR7 and TLR9 agonists respectively, enhanced the antitumor response and cured mice with established ectopic SC TC-1 tumors.⁶ Therefore, using the CH orthotopic model, we compared the antitumor effects of IC and ID pVLP-E7 vaccinations in combination with these adjuvants at days.^{7–9–11} Interestingly, when combined with adjuvants, IC and ID vaccinations resulted in a significant therapeutic effect on the tumor growth, as compared to non-treated mice, whereas adjuvants alone only had a slight, albeit non-significant, effect (Fig. 4A). Furthermore, IC vaccinations combined with adjuvants gave rise to a significant ($p < 0.05$) and better long-term tumor-free survival (58%), as compared

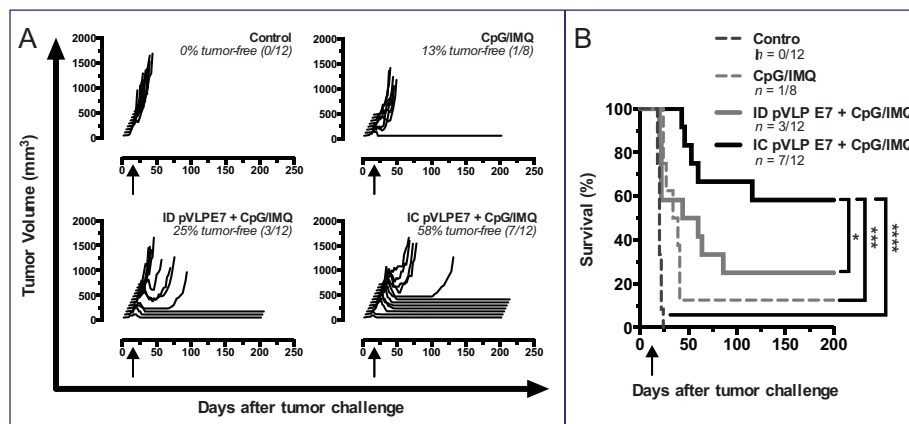


Figure 4. Adjuvants enhanced the therapeutic antitumor effects of intra-cheek vaccinations. C57BL/6 mice bearing intra-cheek TC-1-Luc tumors were ID or IC immunized at days 7–9–11 (arrow) with pVLP-E7 in the presence of adjuvants: CpG-ODN + Imiquimod (CpG/IMQ). As controls, one group of mice received CpG/IMQ alone and another received PBS. (A) Monitoring of tumor volume measured every 2–4 d; tumor-free rates are indicated in italic letters. (B) Kaplan–Meier curves showing tumor-free survival rates. Presented data are pooled from three separate experiments using 3–4 mice per group. * $p < 0.05$; *** $p < 0.001$; **** $p < 0.0001$.

to ID vaccinations combined with adjuvants (25%), for at least 200 d (Fig. 4B). These data confirmed the therapeutic advantage of IC vaccinations over ID route.

Intra-cheek therapeutic effects correlates with better specific CD8⁺ T-cell responses

Whether stronger antitumoral responses obtained after IC vaccinations + adjuvants, as compared to ID vaccinations + adjuvants, could be explained by higher CD8⁺ specific immune responses was then studied. For this purpose, CH tumor-bearing mice were pVLP-E7 vaccinated in combination with adjuvants at days 7–9–11, and then CD8⁺ T cell responses were analyzed in cell suspensions obtained from tumors and TdLNs at day 18. Fig. 5A (upper left panel) shows that IC vaccinations in association with adjuvants induced a significant increase of the absolute number of total CD8⁺ T cells in TdLNs as compared to the ID route + adjuvants ($p < 0.05$), adjuvants alone ($p < 0.01$) or non-vaccinated mice ($p < 0.0001$). In tumors (Fig. 5A, lower left panel), IC and ID vaccination + adjuvants significantly increased the CD8⁺ T-cell density ($p < 0.0001$ and $p < 0.05$, respectively), as compared to non-vaccinated mice. The presence of CD8⁺ specific T cells was further examined using H2-Db E7 tetramers. Significant higher numbers of E7-specific CD8⁺ T cells were found in TdLNs (Fig. 5A, upper middle panel), and in tumors (Fig. 5A lower middle panel) when mice were vaccinated using the IC route and adjuvants. This was accompanied by a slight increase of the percentage of E7-tetramer⁺ cells within tumor infiltrating CD8⁺ T cells (Fig. 5A4). The fact that IC vaccinations induced a higher mobilization of E7-specific cells was confirmed by IFN γ ELISpot Assay (Fig. 5B). To explain this preferential recruitment of CD8⁺ T cells at the mucosal site after IC vaccination, we analyzed the expression of the CD49a integrin, known to be particularly expressed by mucosal T cells.⁹ IC vaccinations demonstrated their superiority comparatively to ID vaccinations to induce E7-specific mucosal CD8⁺ T cells in TdLNs (Fig. 5A, upper right panel) and in tumors (Fig. 5A, lower right panel).

Overall, our findings indicate that the better antitumor efficiency observed after IC vaccinations correlates with higher specific immune responses in TdLNs and tumor

microenvironment. Because the presence of Treg in these sites may be a major hurdle for the efficacy of effector specific T cells to eradicate tumors, we wondered whether our vaccine strategy may or not diminish the density of Treg and/or the balance between Treg and effector T cells. In tumor microenvironment of vaccinated and non-vaccinated mice, the densities of CD4⁺ T cells and Treg did not significantly changed (Fig. 5C, upper left and right panels). Interestingly, the percentage of Treg within CD4⁺ T cells as well as the ratio between Treg and effector T cells (CD4⁺ + CD8⁺ cells) were significantly lower, in all groups of vaccinated mice (including the adjuvant group) by comparison to non-vaccinated mice (Fig. 5C, lower left and right panels). A representative FACS analysis of Treg in tumor infiltrating CD4⁺ cells is shown in the Fig. S4B. Since our data suggest that the antitumor efficiency of IC vaccinations may be due to the recruitment of CD8⁺ effector T cells rather than to those of CD4⁺ effector T cells, we studied the effect of anti-CD8⁺ depleting mAbs prior and during IC vaccinations in tumor-bearing mice. Interestingly, in CD8⁺-depleted mice the antitumor efficiency of IC vaccinations completely disappeared (Fig. 5D), confirming the crucial role of CD8⁺ T cells in the therapeutic effect of IC vaccinations.

Long-term protection effects of intra-cheek vaccinations against tumor relapses

Because of the high relapse rate of HNSCC, that more often occur locally or loco-regionally, it will be of importance that therapeutic vaccines induce long-term protections. For this purpose, mice showing a total regression of TC-1-Luc tumors after vaccination using ID ($n = 3/12$ mice) or IC route ($n = 7/12$ mice) were rechallenged at day 200 with 5×10^4 TC-1-Luc cells injected into the contralateral CH with regard to the initial tumor development. A group of naive mice receiving TC-1-Luc cells was used as tumor growth control. All cured mice were protected from TC-1-Luc tumor cell growth and could survived at least for 400 d (Fig. 6A). Moreover, to study memory responses, specific E7 CD8⁺ T cells were evaluated by using H2-Db-E7 tetramers in the blood of mice 6 weeks after rechallenge. A representative analysis of circulating E7-tetramer⁺ CD8⁺ T cells

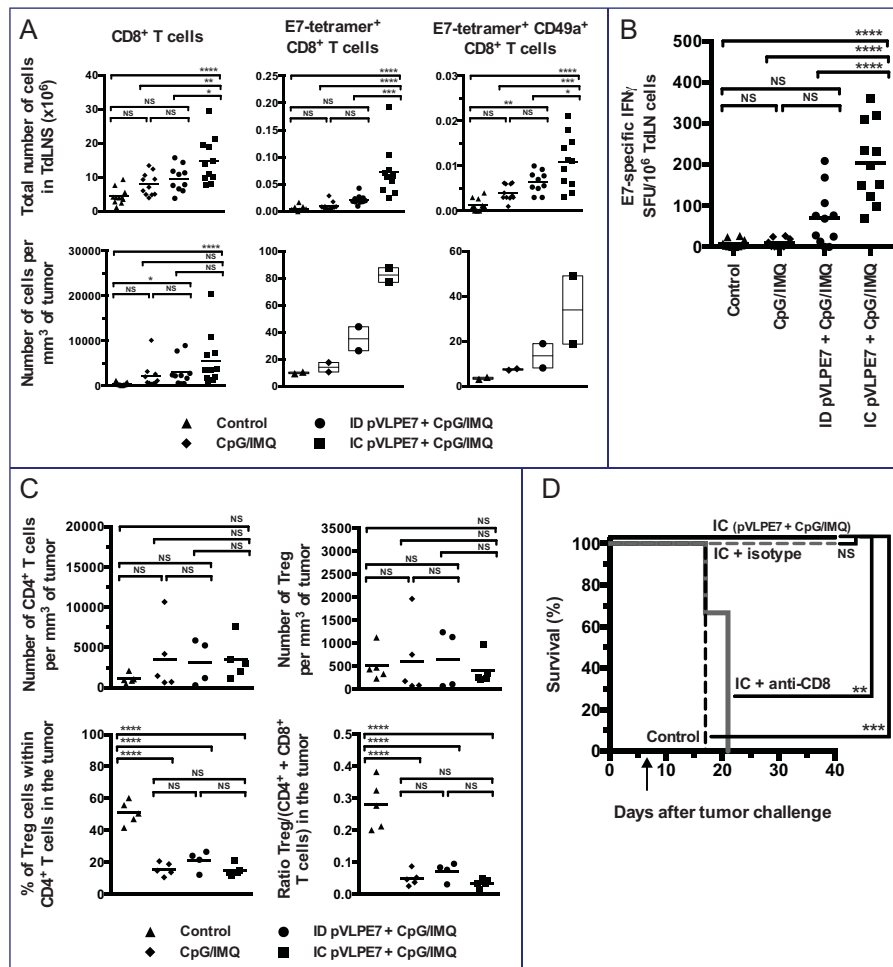


Figure 5. The therapeutic effect of intra-cheek vaccinations correlates with high specific CD8⁺ T-cell responses. C57BL/6 mice bearing intra-cheek TC-1-Luc tumors were ID or IC immunized at days 7–9–11 with pVLP-E7 in the presence of adjuvants: CpG-ODN + Imiquimod (CpG/IMQ). As controls, one group of mice received CpG/IMQ alone and another received PBS. (A) Detection by flow cytometry of E7-tetramer⁺ cells in single cell suspensions obtained from TdLNs and tumors pooled from 5 mice (Experiment 1) and 6 mice (Experiment 2) at day 18. Numbers of E749-57-tetramer⁺, CD8⁺ and CD49a⁺ expressing cells/mm³ (tumors) and per $\times 10^6$ cells (TdLNs) are presented. Presented data were obtained from two separate experiments using 5 and 6 mice, respectively. (B) E7-specific IFN γ ELISpot assay: cells from TdLNs were loaded and stimulated with E749-57 peptide and spot numbers are expressed by 10⁶ cells. The background (always ≤ 100 spots per 10⁶ cells) obtained with not pulsed cells has been subtracted. Presented data are pooled from two separate experiments using 5 and 6 mice per group, respectively. (C) Number of CD4⁺ T cells per mm³ of tumor (upper left panel), number of Treg per mm³ of tumor (upper right panel), percent of Treg in CD4⁺ cells in tumor (lower left panel) and ratio Treg/T effector cells (CD4⁺ and CD8⁺ T cells) in tumor (lower right panel) are shown. (D) Effect of the *in vivo* CD8⁺ depletion in C57BL/6 mice bearing intra-cheek TC-1-Luc tumors when IC immunized with pVLP-E7 combined with CpG/IMQ at days 7–9–11 (arrow). One week before the first vaccination and then once a week, mice received anti-CD8⁺ mAb (100 mg, intraperitoneally) or isotype-matched control mAb. Kaplan–Meier curves showing tumor-free survival rates. NS, non-statistical difference = $p > 0.05$; * $p < 0.05$; ** $p < 0.01$; *** $p < 0.001$; **** $p < 0.0001$.

shows that IC vaccinated mice have a much higher percentage (Mean for 7 mice: $2.09 \pm 0.08\%$, Max = 4.96%) than the ID group (Mean for 3 mice: $0.51 \pm 0.38\%$, Max = 0.93%) or naïve mice (Mean for 7 mice: $0.11 \pm 0.01\%$, Max = 0.17%) (Fig. 6B). Furthermore, central memory and effector memory CD8⁺ T cells were distinguished using CD44 and CD62L markers. In the vaccinated groups, CD8⁺CD44⁺CD62L^{high} (central memory) and CD8⁺CD44⁺CD62L^{low} (effector memory) E7-specific CD8⁺ T cells could be detected (Fig. 6C). Interestingly, IC vaccinations as compared to ID vaccinations induced higher percentage of central memory ($1.49 \pm 0.62\%$, $n = 7$ vs. $0.18 \pm 0.09\%$, $n = 3$) and of effector memory ($0.51 \pm 0.20\%$, $n = 7$ vs. $0.15 \pm 0.06\%$, $n = 3$) E7-specific CD8⁺ T cells. Noteworthy, the percentage of E7-specific mucosal (CD49a⁺) CD8⁺ T cells still remained much higher in rechallenged mice previously vaccinated by the IC route ($1.76 \pm 0.75\%$, $n = 7$), as compared to those vaccinated by the ID route ($0.33 \pm 0.18\%$, $n = 3$) (Fig. 6C, right panel). Overall, our findings indicate that IC

vaccination gave rise to a long-term antitumor response, to better central memory and effector memory specific responses, and to a better recruitment of mucosal effector CD8⁺ T cells, as compared to ID vaccinations.

Discussion

Because prognosis of HNSCC remains poor with a high risk of local recurrence, it is very important to develop therapeutic strategies that aim at eliciting both systemic and local immune responses in order to induce tumor regression and to avoid tumor relapse, thanks to long-term protection. Deciphering tumor microenvironment is crucial to understand the tumor development and to develop immune-based therapies. Indeed, tumors occurring at different anatomical sites differ in their microenvironmental content and may vary in their response to immunotherapy, suggesting that normal tissue surrounding the tumor site can have a decisive role in determining its

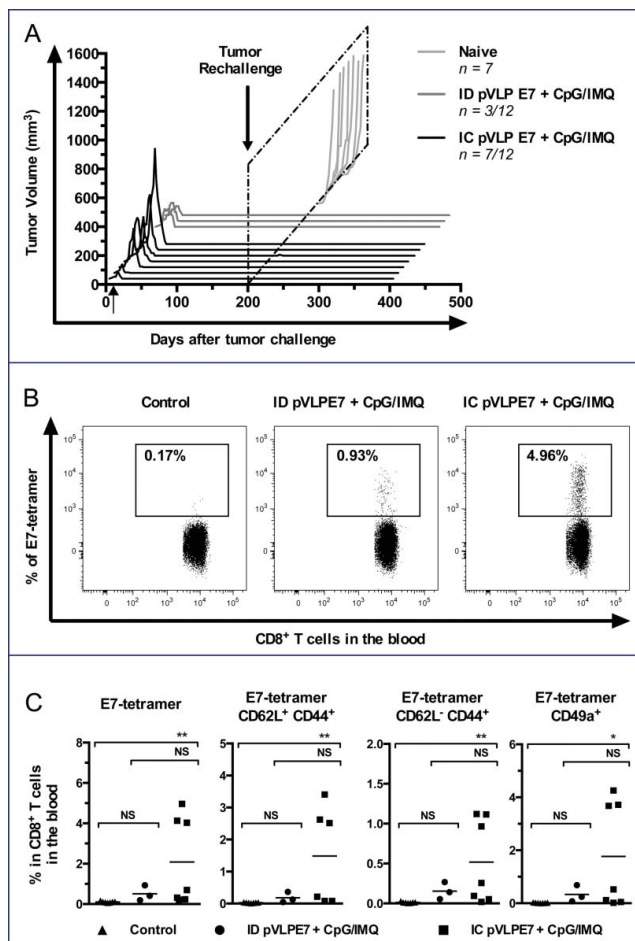


Figure 6. Long-term protection induced by intra-cheek vaccinations. Immunized C57BL/6 mice showing complete tumor regression (3–7 mice per group), were rechallenged with TC-1 cells at day 200. (A) Monitoring of tumor volume measured every 2–4 d. (B) Blood detection by flow cytometry of E749–57-tetramer expressing cells in CD8⁺ T cells at day 250. A representative analysis is shown. (C) Percentages of CD62L, CD44 and CD49a cells in CD8⁺ T cells. Data was obtained from three separate experiments. NS, non-statistical difference = $p > 0.05$; * $p < 0.05$; ** $p < 0.01$.

composition.¹⁰ Moreover, in HNSCC the degree of leukocyte infiltration appears to be dependent upon the tumor site (OSCC or OPSCC) and is likely to be influenced by the differing microenvironments and the stage of the tumor.^{11–13} Our data showing an increased numbers of both innate and adaptive cells in gingivobuccal carcinoma, comparatively to human normal gingiva are in line with other reports showing the inflammatory nature of these cancers.¹⁴ In order to evaluate immunotherapy strategies, such as therapeutic vaccines, development of orthotopic models which provide specific interactions between cancer cells and their native microenvironment¹⁵ is crucial. Because inducible oral-specific tumor models imply labor-intensive processes,^{16,17} we chose to develop orthotopic tumor models using cell lines. Few orthotopic models have been described using syngeneic murine cell line derived from oral cancer^{18–20} or using TC-1 cells.^{9,21} Although we tested the injection of cells in the basis of the tongue as described,⁹ considering the risk of early death and the difficulty of monitoring IL tumor in mice,²² we decided to inject TC-1-Luc cells into the mucosa of the CH, as published by others.²³ Interestingly, we observed significant increases of both innate and adaptive immune cells in the microenvironment of IC

tumors as compared to ectopic TC-1-Luc tumors. This observation was reproduced using the NR-S1 cell line that originates from a spontaneous murine oral carcinoma. Thus, our CH tumor models (TC-1 and NR-S1) display immune cell infiltration features close to those observed in patients with OSCCs, and represent adequate pre-clinical models for oral HNSCCs.

In a context of strong loco-regional risks of recurrence, the orthotopic model allows to study in the same territory, mucosal routes of vaccination and their loco-regional responses. Indeed, mucosal routes possess the advantage over the parenteral route of eliciting local and systemic T-cell responses as well as humoral responses.²⁴ Most of mucosal routes that have been studied are vaginal, rectal or sublingual routes. Sublingual immunotherapy has been widely used for therapeutic allergy vaccines.²⁵ Although several studies have showed the efficiency of the sublingual route to induce tolerance, others have observed cell-mediated immune responses against pathogens,^{26–29} or tumors.³⁰ Similarly, Sandoval et al. have reported that the IN route was able to induce good antitumoral responses in a model of oral cancer and lung.⁹ However, IN immunizations with pVLPs, which require PEI for IN immunization,²⁴ did not promote in our hands detectable immune responses against HPV-16 E7 oncoprotein. More interestingly, we have shown that the IC vaccinations can induce better immune and antitumoral responses particularly in TdLNs, as compared to ID vaccinations. Although no studies have used buccal route for antitumoral vaccination, good immune responses have already been observed against different pathogens.^{31,32} Indeed, humoral and cellular responses against the influenza virus nucleoprotein (NP) of influenza H1N1 have been observed using DNA vaccination associated with electroporation.³² Oral mucosa appears to be an attractive site for vaccine delivery due to their accessibility, anatomy and physiology. In addition, several studies revealed the buccal epithelium as an inductive site for efficient priming of CD8⁺ T lymphocytes.^{31,33} CH localization, contrary to sublingual and IN routes, easily allows the use of electroporation, necessary when using a DNA strategy. Furthermore, the relatively high frequency of DCs, in particular of Langerhans cells and the low numbers of mast cells in human³⁴ in the buccal region makes the CH mucosa an attractive site for vaccine delivery.

Previously, we have shown that the combination of intradermic pVLP vaccinations with adjuvants, such as Imiquimod and CpG-ODN, improved tumor growth inhibition.⁶ Here, we observed that IC vaccinations using the same strategy were even better than ID vaccinations for inducing tumor regression in an orthotopic model of oral cancer. Interestingly, IC route was able to induce a dramatic local and loco-regionally increase of the E7-specific CD8⁺ T cells. It is important to highlight that adjuvants by themselves, when added topically, significantly decreased Treg and the Treg/effectors cells ratio in the tumor microenvironment (see Fig. 5C). This may explain the antitumor efficiency of pVLP vaccinations combined with adjuvants, as compared to pVLP vaccinations alone. Moreover, we demonstrated that IC vaccinations favored a preferential recruitment of antigen-specific CD8⁺ T cells expressing the mucosal integrin CD49a in tumor microenvironment and TdLNs (Fig. 5A). Interestingly, in a previous report Sandoval et al. also observed an increase of specific CD49a⁺ CD8⁺ T cells in IL tumors after IN mucosal vaccination.⁹ Then, these data and

ours suggest a link between IN or IC vaccination and the induction of a mucosal homing program on CD8⁺ T cells that controlled their trafficking. This hypothesis has been also suggested by others.³⁵ Recently, in an orthotopic TC-1 cervical model, it has been shown that cervico-vaginal vaccinations using HPV-16 E7 DNA and HPV E6/E7 recombinant vaccinia induced better specific mucosal CD8⁺ responses and control of TC-1 cervical tumors than intramuscular delivery.³⁶ Thus, mucosal vaccination routes will be of great importance for therapeutic vaccines designed to treat mucosal cancers.

Overall, our findings have shown the advantage of an oral mucosal route of vaccination to induce long-term antitumoral responses by using plasmid-retroviruses as vaccine vectors for antigen delivery and by using a new pre-clinical orthotopic model of oral cancer. In this report, E7 oncoprotein was used as an antigen model applicable for HPV-related HNSCCs. Then, it will be worthwhile to validate our vaccine strategy using pVLPs carrying other tumor-associated antigens particularly involved in non HPV-related HNSCCs.³⁷ Our data are encouraging to rapidly envision a clinical trial for HNSCC because pVLPs, like DNA vaccine, are easy to produce under good manufacturing procedures and the adjuvants used, i.e. CpG-ODN and Imiquimod, are already available as clinical grade reagents. Such vaccine-based clinical trials would be proposed after tumor mass reduction using standard chemo/radiotherapy, known to induce immunological cell death,³⁸ in combination with immune checkpoint inhibitors like PD-1/PD-L1 and/or anti-CTLA4 mAbs.^{39,40}

Material and methods

Human samples

Tumors samples were obtained during surgical resection of primary OSCCs (Maxillofacial Surgery department, Pitié-Salpêtrière Hospital; Paris, France). Gingival tissues were collected from healthy subjects undergoing preventive wisdom tooth extraction (Odontology department, Pitié-Salpêtrière Hospital; Paris, France). Samples were obtained after informed written consent according to local ethic committee authorization.

Mice

Seven- to 8-week-old female C57BL/6J (H-2b) or C3H/HeNRj (H-2k) mice were purchased from Janvier (Le Genest Saint Isle, France) and kept under specific pathogen-free conditions at the UMS28 animal facility (UFR 969, Pitié-Salpêtrière). Experiments were performed according to the European Economic Community guidelines and approved by local ethics committee.

Cell lines

TC-1 cells (CRL-2785; American Type Culture Collection [ATCC]) have been previously described.⁶ TC-1-Luc cells (a generous gift from T.C. Wu, John Hopkins University, MD, USA) were genetically engineered to express the luciferase protein. NR-S1 cells (kindly provided by Dr K. Ando, National

Institute of Radiological Science, Tokyo, Japan), derived from a spontaneous oral carcinoma in C3H mice.⁸

In vivo tumor monitoring

C57BL/6 mice were injected with 5.104 TC-1-Luc cells either SC in the flank, in the CH or IL. C3H/HeNRj mice were injected with 5×10^6 NR-S1 using the SC or IC route. All mice were anesthetized before tumor graft as previously described.⁶ Mice were monitored every 2–3 d for tumor progression and individual weight. Tumor growth was determined using a caliper and according to the formula: $(\text{length} \times \text{width}^2)/2$. For monitoring luciferase activity, mice were intraperitoneally injected with D-luciferin (150 mg/kg) (Promega), bioluminescence images were acquired using IVIS Spectrum (Caliper Life Sciences) and luciferase expression was analyzed with the Living Image 4.2 software (Caliper Life Sciences). Mice were sacrificed when tumors reached volumes of 700–900 mm³ (CH) or 1400–1600 mm³ (SC), or when body weight loss was more than 15% IL.

Tissue analysis by flow cytometry

Human cell suspensions were obtained from tumor and gingival samples after non-enzymatic digestion using Cell Recovery Solution (Corning) at 4°C for 1 h. After filtering, washing and counting, cells were stained with Fixable Viability Dye eFluor780 (eBioscience) at 2–8°C for 30 min. Murine cell suspensions were obtained from tumors, lymph nodes or spleen by enzymatic dissociation using 1 mg/mL of collagenase IV (Sigma-Aldrich) and 0.2 mg/mL of DNase (Roche). After counting cells, they were stained using Fixable Viability Dye eFluor[®]780 at 2–8°C during 10 min. Human or murine cell suspensions were incubated with monoclonal antibodies (mAbs) (Table S1) at 4°C during 20 min, and permeabilized with Foxp3/TFs Staining Buffer Set (eBioscience) for intracellular staining, according to manufacturer's instructions. Acquisition and data analyses were performed using LSRII flow cytometer (Becton Dickinson) and FlowJo v8.8.7 software (TreeStar).

Immunization of mice using pVLP-E7

C57BL/6J mice were immunized using the ID, IC or IN routes, three times at 2-d intervals using pVLP-E7. The structure of the vaccine is composed of two plasmid DNA: pXD01-ΔE7, a plasmid containing a gag-ΔE7 cassette under the control of the human CMV promoter which was obtained from pXD01 and from the pET-15bE7 plasmid that codes for a non-oncogenic deleted 21–26 HPV-16 E7 protein inactivated at the retinoblastoma (Rb) binding motif (ΔE7), and pMΔ2G (kindly provided by D. Trono, Swiss Federal Institute of Technology, Lausanne, Switzerland) a plasmid coding for the vesicular stomatitis virus-G (VSV-G) envelope protein.⁶ Injection of both plasmids leads to the *in vivo* formation of retrovirus-based virus-like particles that display E7 antigen into Gag proteins pseudotyped with VSV-G envelope glycoproteins. For ID and IC immunization, 10 μg pVLP-E7 (7.5 μg pGag-E7 + 2.5 μg pVSV-G) in 40 μL of 0.5% NaCl were injected using the ID route (lower back) or the IC

route (submucosally into the CH inner face) and immediately electroporated in both injection sites using a BTX ECM830 generator (Harvard Apparatus) and CUY650 P3 electrodes (Sonidel limited) as previously described.⁶ For IN immunization, 10 μ g pVLP-E7 in 50 μ L of 5% glucose with PEI-formulated (Ozyme) were administrated slowly into one nostril.²⁴ As control groups, mice were ID or IC injected with 20 μ g of E743-57 (GQAEP-DRAHYNIVTF) polypeptide (Polypeptide Laboratories) mixed with 50 μ g of CpG oligodeoxynucleotides (CpG-ODN, Li28-Lite-nimod, kindly provided by AF. Carpentier). In some groups, pVLP-E7 vaccination was combined with Imiquimod (5 mg/mice, Aldara 5%, MedaPharma) used as a topical treatment and CpG-ODN directly injected (50 μ g CpG-ODN in 50 μ L of 0.9% NaCl) into the periphery of tumors. All mice were anesthetized before immunizations.

ELISpot assays

E7-specific IFN γ production by splenocytes and lymph node cells was determined as follows: briefly, cells (5×10^5 cells/well) were stimulated at 37°C in 5% CO₂ for 24 h with 5 μ g/mL of H-2Db-restricted immunodominant HPV-16 E749-57 peptide (RAHY-NIVTF) (Anaspec). After revelation, spots were counted using the AID ELISpot reader (ELR03, AID Autoimmun Diagnostika). Results are presented as the mean of triplicate wells, and numbers of spots are expressed for 10⁶ cells.

Tetramer staining

For the detection of infiltrating E7-specific CD8⁺ T cells, tumors and TdLNs cells were dissociated as described above, and CD8⁺ cells were purified by MACS using anti-CD8⁺ microbeads (Miltenyi Biotec). Cells were stained with CD45, CD3e, CD8a, CD49a mAbs (all from Biosciences) and E749-57/Db Tetramers (Beckman Coulter). Then, tubes were incubated 20–30 min in the dark at room temperature, and analyzed by flow cytometry.

In vivo CD8⁺ T-cell depletion

To evaluate the role of CD8⁺ T cells in the antitumor effect, CD8⁺ T cells were *in vivo* depleted as follows: 100 μ g of anti-CD8⁺ mAbs (rat IgG2b mAb, clone YTS 169.4 from Proteogenix) per mice or isotype control mAbs were intraperitoneally injected one week before therapeutic vaccination and then once a week as previously described.⁹

Antitumoral long-term protection

IC or ID vaccinated mice showing complete tumor regression at day 200, were orthotopically rechallenged with 5×10^4 TC-1 cells. Naive mice were used as controls. Mice were monitored as described above for tumor progression up to day 400. At day 250, blood (300–350 μ L) was collected by retro-orbital puncture into heparinized tubes. Peripheral blood mononuclear cells (PBMC) were isolated by density gradient centrifugation using LSA 1077 (PAA). PBMC were stained with CD3e, CD8a, CD49a mAbs (all from Biosciences), CD4⁺, CD44, CD62L

mAbs (all from Biologend) and E749-57/Db Tetramers as described above, and then analyzed by flow cytometry.

Statistical Analyses

Student *t*-test or one-way ANOVA with Tukey's correction was used for normally distributed data. Mann–Whitney or Kruskal–Wallis with Dunn's correction were used for non parametric data. Kaplan–Meier log-rank analysis was used to evaluate the survival differences between groups. Statistical analysis was conducted using Prism 6.0 software (GraphPad). Only *p* values < 0.05 were considered as significant. Results are presented as mean (linear data) or geometric mean (logarithmic data) \pm SEM of *n* separate experiments.

Disclosure of potential conflicts of interest

No potential conflicts of interest were disclosed.

Acknowledgments

The authors thank the Fondation ARC pour la Recherche sur le Cancer, and La Ligue Nationale contre le Cancer for supporting financially this work. RM thanks the Association pour la Recherche sur la Moelle Osseuse (ARMO) for his fellowship. JR thanks INSERM for a one-year fellowship. JR and KT thank the Fondation “Les Gueules Cassées” who partly supported them with fellowships.

Funding

This work was financially supported by grants from Fondation ARC pour la Recherche sur le Cancer and La Ligue Nationale contre le Cancer. RM received a fellowship from the Association pour la Recherche sur la Moelle Osseuse (ARMO). JR received a one-year fellowship from INSERM. JR and KT were partly supported by the Fondation “Les Gueules Cassées.”

Author Contributions

Conception and design: R. Macedo, G. Lescaille, F.M. Lemoine. Development of methodology: R. Macedo, J. Rochefort, M. Guillot-Delost, B. Bellier, V. Mateo, A.F. Carpentier, E. Tartour, G. Lescaille, F.M. Lemoine. Acquisition of data (provided animals, acquired and managed patients, provided facilities, etc.): R. Macedo, J. Rochefort, M. Guillot-Delost, K. Tanaka, A. Le Moignic, C. Noizat, C. Baillou, V. Mateo, E. Tartour, C. Bertolus, G. Lescaille, F.M. Lemoine. Analysis and interpretation of data (e.g. statistical analysis, biostatistics, computational analysis): R. Macedo, J. Rochefort, M. Guillot-Delost, B. Bellier, V. Mateo, G. Lescaille, F.M. Lemoine. Writing, review, and/or revision of the manuscript: R. Macedo, M. Guillot-Delost, E. Tartour, B. Bellier, G. Lescaille, F.M. Lemoine. Administrative, technical, or material support (i.e. reporting or organizing data, constructing databases): R. Macedo, J. Rochefort, M. Guillot-Delost, B. Bellier, G. Lescaille, F.M. Lemoine. Study supervision: G. Lescaille, F.M. Lemoine.

References

1. Islami F, Fedirko V, Tramacere I, Bagnardi V, Jenab M, Scotti L, Rota M, Corrao G, Garavello W, Schuz J et al. Alcohol drinking and esophageal squamous cell carcinoma with focus on light-drinkers and never-smokers: a systematic review and meta-analysis. *Int J Cancer J Int Du Cancer* 2011; 129:2473-84; PMID:21190191; <http://dx.doi.org/10.1002/ijc.25885>
2. Tramacere I, Negri E, Bagnardi V, Garavello W, Rota M, Scotti L, Islami F, Corrao G, Boffetta P, La Vecchia C. A meta-analysis of alcohol

- drinking and oral and pharyngeal cancers. Part 1: overall results and dose-risk relation. *Oral Oncol* 2010; 46:497-503; PMID:20444641; <http://dx.doi.org/10.1016/j.oraloncology.2010.03.024>
3. Majchrzak E, Szybiak B, Wegner A, Pienkowski P, Pazdrowski J, Luczewski L, Sowka M, Golusinski P, Malicki J, Golusinski W. Oral cavity and oropharyngeal squamous cell carcinoma in young adults: a review of the literature. *Radiol Oncol* 2014; 48:1-10; PMID:24587773; <http://dx.doi.org/10.2478/raon-2013-0057>
 4. Fakhry C, Psyrris A, Chaturvedi A. HPV and head and neck cancers: state-of-the-science. *Oral Oncol* 2014; 50:353-5; PMID:24726207; <http://dx.doi.org/10.1016/j.oraloncology.2014.03.010>
 5. Ho AS, Kraus DH, Ganly I, Lee NY, Shah JP, Morris LG. Decision making in the management of recurrent head and neck cancer. *Head Neck* 2014; 36:144-51; PMID:23471843; <http://dx.doi.org/10.1002/hed.23227>
 6. Lescaille G, Pitoiset F, Macedo R, Baillou C, Huret C, Klatzmann D, Tartour E, Lemoine FM, Bellier B. Efficacy of DNA vaccines forming e7 recombinant retroviral virus-like particles for the treatment of human papillomavirus-induced cancers. *Human Gene Therapy* 2013; 24:533-44; PMID:23521528; <http://dx.doi.org/10.1089/hum.2012.037>
 7. Nizard M, Diniz MO, Roussel H, Tran T, Ferreira LC, Badoual C, Tartour E. Mucosal vaccines: novel strategies and applications for the control of pathogens and tumors at mucosal sites. *Hum Vaccin Immunother* 2014; 10:2175-87; PMID:25424921; <http://dx.doi.org/10.4161/hv.29269>
 8. Usui S, Urano M, Koike S, Kobayashi Y. Effect of PS-K, a protein polysaccharide, on pulmonary metastases of a C3H mouse squamous cell carcinoma. *J Natl Cancer Inst* 1976; 56:185-7; PMID:130494
 9. Sandoval F, Terme M, Nizard M, Badoual C, Bureau MF, Freyburger L, Clement O, Marcheteau E, Gey A, Fraise G et al. Mucosal imprinting of vaccine-induced CD8(+) T cells is crucial to inhibit the growth of mucosal tumors. *Sci Translational Med* 2013; 5:172ra20; PMID:23408053; <http://dx.doi.org/10.1126/scitranslmed.3004888>
 10. Devaud C, Westwood JA, John LB, Flynn JK, Paquet-Fifield S, Duong CP, Yong CS, Pegram HJ, Stacker SA, Achen MG et al. Tissues in different anatomical sites can sculpt and vary the tumor microenvironment to affect responses to therapy. *Mol Therapy* 2014; 22:18-27; PMID:24048441; <http://dx.doi.org/10.1038/mt.2013.219>
 11. Green VL, Michno A, Stafford ND, Greenman J. Increased prevalence of tumour infiltrating immune cells in oropharyngeal tumours in comparison to other subsites: relationship to peripheral immunity. *Cancer Immunol Immunotherapy* 2013; 62:863-73; PMID:23359088; <http://dx.doi.org/10.1007/s00262-013-1395-9>
 12. Wansom D, Light E, Thomas D, Worden F, Prince M, Urba S, Chepeha D, Kumar B, Cordell K, Eisbruch A et al. Infiltrating lymphocytes and human papillomavirus-16-associated oropharyngeal cancer. *Laryngoscope* 2012; 122:121-7; PMID:22183632; <http://dx.doi.org/10.1002/lary.22133>
 13. Wolf GT, Chepeha DB, Bellile E, Nguyen A, Thomas D, McHugh J. Tumor infiltrating lymphocytes (TIL) and prognosis in oral cavity squamous carcinoma: a preliminary study. *Oral Oncol* 2014; 51:90-5; PMID:25283344; <http://dx.doi.org/10.1016/j.oraloncology.2014.09.006>
 14. Wallis SP, Stafford ND, Greenman J. Clinical relevance of immune parameters in the tumor microenvironment of head and neck cancers. *Head Neck* 2014; 37:449-59; PMID:24803283; <http://dx.doi.org/10.1002/hed.23736>
 15. McMillin DW, Negri JM, Mitsiades CS. The role of tumour-stromal interactions in modifying drug response: challenges and opportunities. *Nat Rev Drug Discov* 2013; 12:217-28; PMID:23449307; <http://dx.doi.org/10.1038/nrd3870>
 16. Tang XH, Knudsen B, Bemis D, Tickoo S, Gudas LJ. Oral cavity and esophageal carcinogenesis modeled in carcinogen-treated mice. *Clin Cancer Res* 2004; 10:301-13; PMID:14734483; <http://dx.doi.org/10.1158/1078-0432.CCR-0999-3>
 17. Raimondi AR, Molinolo A, Gutkind JS. Rapamycin prevents early onset of tumorigenesis in an oral-specific K-ras and p53 two-hit carcinogenesis model. *Cancer Res* 2009; 69:4159-66; PMID:19435901; <http://dx.doi.org/10.1158/0008-5472.CAN-08-4645>
 18. Cui N, Nomura T, Noma H, Yokoo K, Takagi R, Hashimoto S, Okamoto M, Sato M, Yu G, Guo C et al. Effect of YM529 on a model of mandibular invasion by oral squamous cell carcinoma in mice. *Clin Cancer Res* 2005; 11:2713-9; PMID:15814653; <http://dx.doi.org/10.1158/1078-0432.CCR-04-1767>
 19. Vahle AK, Hermann S, Schafers M, Wildner M, Kerem A, Ozturk E, Jure-Kunkel M, Franklin C, Lang S, Brandau S. Multimodal imaging analysis of an orthotopic head and neck cancer mouse model and application of anti-CD137 tumor immune therapy. *Head Neck* 2016; 38(4):542-9; PMID:25482887; <http://dx.doi.org/10.1002/hed.23929>
 20. Paolini F, Massa S, Manni I, Franconi R, Venuti A. Immunotherapy in new pre-clinical models of HPV-associated oral cancers. *Hum Vaccin Immunother* 2013; 9:534-43; PMID:23296123; <http://dx.doi.org/10.4161/hv.23232>
 21. Mondini M, Nizard M, Tran T, Mauge L, Loi M, Clemenson C, Dugue D, Maroun P, Louvet E, Adam J et al. Synergy of Radiotherapy and a Cancer Vaccine for the Treatment of HPV-Associated Head and Neck Cancer. *Mol Cancer Therapeutics* 2015; 14:1336-45; PMID:25833837; <http://dx.doi.org/10.1158/1535-7163.MCT-14-1015>
 22. Bozec A, Sudaka A, Toussan N, Fischel JL, Etienne-Grimaldi MC, Milano G. Combination of sunitinib, cetuximab and irradiation in an orthotopic head and neck cancer model. *Annals Oncol* 2009; 20:1703-7; PMID:19542251; <http://dx.doi.org/10.1093/annonc/mdp070>
 23. Yang K, Zhao N, Zhao D, Chen D, Li Y. The drug efficacy and adverse reactions in a mouse model of oral squamous cell carcinoma treated with oxaliplatin at different time points during a day. *Drug Des Devel Ther* 2013; 7:511-7; PMID:23818762; <http://dx.doi.org/10.2147/DDDT.S46323>
 24. Torrieri-Dramard L, Lambrecht B, Ferreira HL, Van den Berg T, Klatzmann D, Bellier B. Intranasal DNA vaccination induces potent mucosal and systemic immune responses and cross-protective immunity against influenza viruses. *Mol Therapy* 2011; 19:602-11; PMID:20959813; <http://dx.doi.org/10.1038/mt.2010.222>
 25. Mascarell L, Zimmer A, Van Overtvelt L, Tourdot S, Moingeon P. Induction of allergen-specific tolerance via mucosal routes. *Curr Top Microbiol Immunol* 2011; 352:85-105; PMID:21562971; http://dx.doi.org/10.1007/82_2011_132
 26. Appledorn DM, Aldhamen YA, Godbehere S, Seregin SS, Amalfitano A. Sublingual administration of an adenovirus serotype 5 (Ad5)-based vaccine confirms Toll-like receptor agonist activity in the oral cavity and elicits improved mucosal and systemic cell-mediated responses against HIV antigens despite preexisting Ad5 immunity. *Clin Vaccine Immunol* 2011; 18:150-60; PMID:21084461; <http://dx.doi.org/10.1128/CVI.00341-10>
 27. Choi JH, Schafer SC, Zhang L, Kobinger GP, Juelich T, Freiberg AN, Croyle MA. A single sublingual dose of an adenovirus-based vaccine protects against lethal Ebola challenge in mice and guinea pigs. *Mol Pharm* 2012; 9:156-67; PMID:22149096; <http://dx.doi.org/10.1021/mp200392g>
 28. Domm W, Brooks L, Chung HL, Feng C, Bowers WJ, Watson G, McGrath JL, Dewhurst S. Robust antigen-specific humoral immune responses to sublingually delivered adenoviral vectors encoding HIV-1 Env: association with mucoadhesion and efficient penetration of the sublingual barrier. *Vaccine* 2011; 29:7080-9; PMID:21801777; <http://dx.doi.org/10.1016/j.vaccine.2011.07.008>
 29. Park HJ, Ferko B, Byun YH, Song JH, Han GY, Roethl E, Egorov A, Muster T, Seong B, Kweon MN et al. Sublingual immunization with a live attenuated influenza A virus lacking the nonstructural protein 1 induces broad protective immunity in mice. *PLoS one* 2012; 7:e39921; PMID:22761928; <http://dx.doi.org/10.1371/journal.pone.0039921>
 30. Singh S, Yang G, Schluns KS, Anthony SM, Sastry KJ. Sublingual vaccination induces mucosal and systemic adaptive immunity for protection against lung tumor challenge. *PLoS one* 2014; 9:e90001; PMID:24599269; <http://dx.doi.org/10.1371/journal.pone.0090001>
 31. Etchart N, Desmoulin PO, Chemin K, Maliszewski C, Dubois B, Wild F, Kaiserlian D. Dendritic cells recruitment and *in vivo* priming of CD8+ CTL induced by a single topical or transepithelial immunization via the buccal mucosa with measles virus nucleoprotein. *J Immunol* 2001; 167:384-91; PMID:11418674; <http://dx.doi.org/10.4049/jimmunol.167.1.384>
 32. Kichaev G, Mendoza JM, Amante D, Smith TR, McCoy JR, Sardesai NY, Broderick KE. Electroporation mediated DNA vaccination directly to a mucosal surface results in improved immune responses. *Hum Vaccin Immunother* 2013; 9:2041-8; PMID:23954979; <http://dx.doi.org/10.4161/hv.25272>

33. Desvignes C, Esteves F, Etchart N, Bella C, Czerkinsky C, Kaiserlian D. The murine buccal mucosa is an inductive site for priming class I-restricted CD8+ effector T cells *in vivo*. *Clin Exp Immunol* 1998; 113:386-93; PMID:9737667; <http://dx.doi.org/10.1046/j.1365-2249.1998.00671.x>
34. Allam JP, Stojanovski G, Friedrichs N, Peng W, Bieber T, Wenzel J, Novak N. Distribution of Langerhans cells and mast cells within the human oral mucosa: new application sites of allergens in sublingual immunotherapy? *Allergy* 2008; 63:720-7; PMID:18445186; <http://dx.doi.org/10.1111/j.1398-9995.2007.01611.x>
35. Hervouet C, Luci C, Bekri S, Juhel T, Bihl F, Braud VM, Czerkinsky C, Anjuere F. Antigen-bearing dendritic cells from the sublingual mucosa recirculate to distant systemic lymphoid organs to prime mucosal CD8 T cells. *Mucosal Immunol* 2014; 7:280-91; PMID:23801305; <http://dx.doi.org/10.1038/mi.2013.45>
36. Sun YY, Peng S, Han L, Qiu J, Song L, Tsai YC, Yang B, Roden RB, Trimble CL, Hung CF et al. Local HPV recombinant Vaccinia boost following priming with an HPV DNA vaccine enhances local HPV-specific CD8+ T cell mediated tumor control in the genital tract. *Clin Cancer Res* 2013; 22(3):657-69; PMID:26420854; <http://dx.doi.org/10.1158/1078-0432.CCR-15-0234>
37. Laban S, Atanackovic D, Luetkens T, Knecht R, Busch CJ, Freytag M, Spagnoli G, Ritter G, Hoffmann TK, Knuth A et al. Simultaneous cytoplasmic and nuclear protein expression of melanoma antigen-A family and NY-ESO-1 cancer-testis antigens represents an independent marker for poor survival in head and neck cancer. *Int J Cancer J Int Du Cancer* 2015; 135:1142-52; PMID:24482145; <http://dx.doi.org/10.1002/ijc.28752>
38. Kroemer G, Galluzzi L, Kepp O, Zitvogel L. Immunogenic cell death in cancer therapy. *Annu Rev Immunol* 2013; 31:51-72; PMID:23157435; <http://dx.doi.org/10.1146/annurev-immunol-032712-100008>
39. Perez-Gracia JL, Labiano S, Rodriguez-Ruiz ME, Sanmamed MF, Melero I. Orchestrating immune check-point blockade for cancer immunotherapy in combinations. *Curr Opin Immunol* 2014; 27:89-97; PMID:24485523; <http://dx.doi.org/10.1016/j.coi.2014.01.002>
40. Badoual C, Hans S, Merillon N, Van Ryswick C, Ravel P, Benhamouda N, Levionnois E, Nizard M, Si-Mohamed A, Besnier N et al. PD-1-expressing tumor-infiltrating T cells are a favorable prognostic biomarker in HPV-associated head and neck cancer. *Cancer Res* 2013; 73:128-38; PMID:23135914; <http://dx.doi.org/10.1158/0008-5472.CAN-12-2606>